

1 **SARS-CoV-2 assays to detect functional antibody responses that block ACE2  
2 recognition in vaccinated animals and infected patients**

3

4

5 Susanne N. Walker<sup>1^\*</sup>, Neethu Chokkalingam<sup>1^\*</sup>, Emma L. Reuschel<sup>1</sup>, Mansi Purwar<sup>1</sup>, Ziyang Xu<sup>1</sup>,  
6 Ebony N. Gary<sup>1</sup>, Kevin Y. Kim<sup>1</sup>, Katherine Schultheis<sup>2</sup>, Jewell Walters<sup>2</sup>, Stephanie Ramos<sup>2</sup>, Trevor  
7 R.F. Smith<sup>2</sup>, Kate E. Broderick<sup>2</sup>, Pablo Tebas<sup>3</sup>, Ami Patel<sup>1</sup>, David B. Weiner<sup>1</sup> and Daniel W. Kulp<sup>1,4\*</sup>

8

9 <sup>1</sup>Vaccine and Immunotherapy Center, Wistar Institute, Philadelphia, PA, 19104, USA

10 <sup>2</sup>Inovio Pharmaceuticals, Plymouth Meeting, PA, 19462, USA

11 <sup>3</sup>Department of Medicine; University of Pennsylvania Perelman School of Medicine,  
12 Philadelphia, PA ,19104, United States.

13 <sup>4</sup>Department of Microbiology, Perelman School of Medicine, University of Pennsylvania,  
14 Philadelphia, PA 19104, United States

15

16

17 \* Corresponding author

18 ^ Authors contributed equally

19    **Abstract**

20    SARS-CoV-2 (Severe Acute Respiratory Syndrome Coronavirus 2) has caused a global  
21    pandemic of COVID-19 resulting in cases of mild to severe respiratory distress and significant  
22    mortality. The global outbreak of this novel coronavirus has now infected >8 million people  
23    worldwide with >2 million cases in the US (June 17<sup>th</sup>, 2020). There is an urgent need for  
24    vaccines and therapeutics to combat the spread of this coronavirus. Similarly, the development  
25    of diagnostic and research tools to determine infection and vaccine efficacy are critically  
26    needed. Molecular assays have been developed to determine viral genetic material present in  
27    patients. Serological assays have been developed to determine humoral responses to the spike  
28    protein or receptor binding domain (RBD). Detection of functional antibodies can be  
29    accomplished through neutralization of live SARS-CoV2 virus, but requires significant expertise,  
30    an infectible stable cell line, a specialized BioSafety Level 3 (BSL-3) facility. As large numbers  
31    of people return from quarantine, it is critical to have rapid diagnostics that can be widely  
32    adopted and employed to assess functional antibody levels in the returning workforce. This type  
33    of surrogate neutralization diagnostic can also be used to assess humoral immune responses  
34    induced in patients from the large number of vaccine and immunotherapy trials currently on-  
35    going. Here we describe a rapid serological diagnostic assay for determining antibody receptor  
36    blocking and demonstrate the broad utility of the assay by measuring the antibody functionality  
37    of sera from small animals and non-human primates immunized with an experimental SARS-  
38    CoV-2 vaccine and using sera from infected patients.

39

40    **Keywords**

41    SARS-CoV-2, COVID-19, ACE2 blocking assay, Serological tests, Functional antibodies,  
42    SARS-CoV-2 vaccine, SARS-CoV-2 immunity

43

44    **Background**

45 The city of Wuhan China became the epicenter for a global pandemic in December of 2019  
46 when the first cases of respiratory illnesses were reported and identified as being caused by a  
47 novel betacoronavirus now referred to as SARS-CoV-2. The novel SARS-CoV-2 virus is closely  
48 related to the SARS-CoV-1 virus and has a high human-to-human transmission rate(1). As of  
49 May 22<sup>nd</sup> 2020, over 5,128,492 people are reported positive for viral infection of SARS-CoV-2  
50 resulting in 333,489 fatalities worldwide(2). SARS-CoV-2 modes of transmission include  
51 shedding of the virions in airborne droplets and close contact. Once infected, people develop  
52 flu-like symptoms and severe cases can lead to acute respiratory distress syndrome (ARDS),  
53 acute respiratory failure, severe pneumonia, pulmonary edema, multiple organ failure and  
54 death. Quarantines around the globe have helped curb spread of the virus and as people are  
55 eager to return to life as normal, development of methods and assays to aid in the detection of  
56 SARS-CoV-2 and effective measurements are of utmost importance.

57

58 Angiotensin-converting enzyme 2 (ACE2) is highly expressed on lung epithelial cells and is the  
59 viral receptor for SARS-CoV-1(3). Recently, ACE2 has also been identified as a receptor utilized  
60 by SARS-CoV-2(4). A 193 amino acid region on the spike protein of SARS-CoV-1 and SARS-  
61 CoV-2 termed the receptor binding domain (RBD) was found to interact with the ACE2 receptor  
62 and primarily mediates cell entry(5-10). Cryo-electron microscopy was used to determine a high  
63 resolution structure of the prefusion spike protein and help define the ACE2 interaction site(11,  
64 12). In the SARS-CoV-1 outbreak of 2003, it was reported that high titers of protecting IgG were  
65 found in the convalescent serum of patients recovering from infection(13). Early studies show  
66 treating COVID-19 patients presenting with severe ARDS with convalescent plasma therapy  
67 (CPT) may be beneficial(14, 15). In order to determine if a recovered patient could be re-  
68 infected or if their plasma may be useful as a treatment to others, assessment of functional  
69 antibody response is highly valuable. While tests for SARS-CoV-2 seropositivity are being  
70 deployed, they do not necessarily correlate with neutralizing immunity(16). As there are limited

71 options for rapid diagnostic of functional antibody responses, fast and simple functional assays  
72 may prove to be a critical assessment tool to discriminate between potential CPT donors.

73

74 In parallel with CPT, major academic, industry and government entities are pushing for  
75 therapeutics and vaccines against SARS-CoV-2. Given this urgent need, there are numerous  
76 clinical vaccine trials underway for SARS-CoV-2 in parallel(17). Through pre-clinical testing,  
77 vaccine-induced functional antibody responses are being used to discriminate among potential  
78 vaccine candidates. In clinical testing, the humoral responses will need to be analyzed for  
79 functionality to assess immunogenicity of each vaccine. Therefore, rapid assays for detecting  
80 functional IgGs in human serum for SARS-CoV-2 are essential to compare vaccine candidates  
81 and to understand induced immunity.

82

83 Early into this pandemic, diagnostic tools for detecting viral genetic material were developed  
84 and utilized in a real-time reverse transcription PCR assay(18). Serologic assays for detecting  
85 anti-SARS-CoV-2 antibodies are now also available(19). However, single antigen ELISA  
86 assays can suffer from detection limits and numbers of false positives(20) and may not be  
87 associated solely with protective responses. Faster and straight forward approaches which  
88 detect specific interactions to reduce false positives are needed. Neutralization assays that can  
89 detect functional immunity have been developed with replicating virus, but require handling in  
90 specialized BSL-3 facilities, severely limiting the number of samples that can be processed.  
91 Pseudovirus neutralization assays run in BSL-2 facilities were quickly developed to detect the  
92 functional antibody response in sera(21). While this is a critical tool for determining protective  
93 antibody titers, it requires several days for a readout and are not standardized between  
94 laboratories. The pseudoviruses produced in these assays are not easily manufactured and  
95 take time to express, harvest, and titer. One such approach to help augment the methods listed  
96 above is an enzyme-linked immunosorbent assay (ELISA) employed in a competitive manner to

97 determine levels of ACE2 receptor blocking antibodies in a sample. In addition, recent advances  
98 of portable and field-deployable surface plasmon resonance (SPR) devices(22) and widespread  
99 availability of SPR instruments in research laboratories make SPR an additional platform for  
100 measuring ACE2 receptor blocking. Here, we describe a competition ELISA assay and a SPR  
101 assay developed to rapidly detect ACE2 receptor blocking antibodies in IgGs and sera of  
102 vaccinated mice, guinea pigs, rabbits and non-human primates, as well as, human samples  
103 from SARS-CoV-2 patients.

104

## 105 **Results**

106

### 107 **Receptor expression and assay development**

108 To detect SARS-CoV-2 spike protein binding to ACE2, we designed a soluble variant of the  
109 membrane-bound human ACE2 receptor. The ectodomain of the receptor was fused to a  
110 human IgG1 Fc tag (ACE2-IgHu), for purification and secondary antibody recognition. This  
111 protein fusion was expressed in mammalian cells to ensure proper glycosylation and purified on  
112 a protein A column. To determine that ACE2-IgHu was dimeric and a homogeneous species in  
113 solution, we employed size exclusion chromatography tandem multi angle light scattering (SEC-  
114 MALS). The SEC trace shows a single peak (Fig. 1A) and the MALS data determined the  
115 estimated molecular weight to be 190 kDa for ACE2-IgHu, which is very close to the expected  
116 molecular weight of a dimer of ACE2-IgHu at 195 kDa (**Fig. 1B**). We next sought to confirm the  
117 functionality of ACE2-IgHu. Previous studies suggest SARS-CoV-2 binds to ACE2 with an  
118 affinity range of 4-34nM(6, 11). We determined that our ACE2-IgHu binds with similar affinity to  
119 the receptor binding domain (RBD) of SARS-CoV-2 spike (27.5nM) as assessed by SPR (**Fig.**  
120 **1C**). Next, using Enzyme-Linked Immunosorbent Assays (ELISAs) we immobilized full-length  
121 SARS-CoV-2 spike protein (containing both the S1 and S2 subunits) and incubated a dilution  
122 series of ACE2-IgHu (**Fig. 1D**). The binding curves confirmed the high affinity interaction of the

123 receptor for the spike protein. We further showed similar binding for two independent batches of  
124 ACE2, as well as a sample that was frozen and thawed (**Fig. S1A**). From the binding curve, we  
125 hypothesized that a reasonable concentration of ACE2 protein fusion needed to see competitive  
126 blocking while still binding >90% of immobilized spike protein in the absence of blocking would  
127 be around 0.1-1 ug/ml (**Fig. 1D, red arrow**).

128 To examine if we could construct a competition assay, we employed ACE2-IgMu (mouse Fc) to  
129 act as a competitor to ACE2-IgHu. To match our initial binding ELISA format, the competition  
130 ELISA assay similarly captured a His6X-tagged full-length spike protein by first immobilizing an  
131 anti-His polyclonal antibody. A dilution series of the competitor (ACE2-IgMu) was pre-mixed with  
132 a constant concentration of soluble receptor (ACE2-IgHu). A secondary anti-human antibody  
133 conjugated to horseradish peroxidase (HRP) determines the amount of ACE2-IgHu present  
134 through a TMB colorimetric readout (**Fig. 2A**). In order to formally determine the optimal  
135 concentration of soluble receptor (ACE2-IgHu), we performed the assay at four concentrations  
136 ranging from 0.01ug/ml to 10 ug/ml (**Fig. 2B**). The ACE2-IgHu concentration of 0.1 ug/ml (red  
137 curve in **Fig. 2B**), was able to show a complete inhibition curve in the presence of ACE2-IgMu.  
138

### 139 **Animal IgG and serological competition**

140 The proof-of-concept competition ELISA displayed a full blocking curve, so we sought to utilize  
141 this assay for animals immunized with SARS-CoV-2 spike protein. The same design for the  
142 competition ELISA was used for this assay, replacing the ACE2-IgMu competitor with antibodies  
143 induced by vaccination (**Fig. 3A**). In our previous work, BALB/c mice were immunized with DNA  
144 plasmids encoding SARS-CoV-2 spike protein(23). To examine the activity of antibodies in the  
145 sera, IgGs from either naïve mice or vaccinated mice 14 days post-immunization were purified  
146 using a protein G column. Unlike the ACE2 control which only binds to the receptor binding site  
147 (RBS) on the receptor binding domain (RBD) of the spike protein, antibodies from immunized  
148 mice can bind to a multitude of epitopes on the spike protein including epitopes on the S1

149 subunit(which includes the RBD), S2 subunit or S1-S2 interfaces. While antibodies distal to the  
150 RBS should have less effect on ACE2 binding, we hypothesized that such distal antibodies may  
151 inhibit ACE2 binding directly by sterically obscuring the RBS or indirectly by causing allosteric  
152 conformational shifts in the spike protein. To test this, we immobilized either the full spike  
153 protein (S1+S2) or S1 alone to examine the levels of detectable blocking antibodies. A mixture  
154 of ACE2-IgHu at a constant concentration of 0.1 ug/ml and a dilution series from a vaccinated  
155 mouse IgG (IgGm1) or naïve mice IgG (naïve IgGm) was incubated on the plate. An anti-  
156 human-HRP conjugated antibody was added to determine the ACE2 binding in the presence of  
157 IgGm. As **Fig. 3B** illustrates, there is greater antibody blocking with the full spike protein than  
158 with the S1 subunit alone (Fig. S2A).

159  
160 To show the utility of this assay in samples from larger mammals, we examined receptor  
161 blocking of rabbit sera from SARS-CoV-2 immunization studies. We pooled sera from five  
162 rabbits two weeks post immunization in 3 groups (low dose of 1mg, high dose of 2mg and  
163 naïve) as well as a Day 0 pool from all 15 animals. The IgG from these pools were purified on a  
164 protein G column and used as competitors in the competition ELISA assay. To compare the  
165 blocking efficacy, the area under the curve (AUC) was calculated for each competition curve.  
166 For full, uninhibited ACE2 binding, the AUC will be larger than the AUC for a competitive curve  
167 (**Fig. 3C**). As seen with the mouse IgGs, the pooled vaccinated rabbit IgG displayed statistically  
168 significant blocking of ACE2 receptor binding compared to the naïve animal pool and the Day 0  
169 pool (**Fig. 3D, Fig S2B**). The high dose rabbits reduced ACE2 signal relative to the low dose  
170 group, highlighting the utility of the assay to help discriminate between different vaccine  
171 regimens. Up to this point we have analyzed purified IgGs collected from sera, however we  
172 wanted to validate the use of this assay on serological samples as well. The same rabbit sera  
173 pools were used as competitors in the competition ELISA assay in a dilution series to compare

174 blocking between sera and purified IgG. The rabbit sera displayed statistically significant ACE2  
175 receptor blocking as we saw in the purified IgG assay (**Fig. 3E, Fig. S2C**).

176

177 Next, we sought to show that we could assess receptor blocking in a third animal model of  
178 guinea pigs which were immunized with a SARS-CoV-2 Spike-based vaccine(23). We  
179 compared a pool of sera collected on day 14 post immunization to a Day 0 pool (**Fig. 3F**). The  
180 immune pool showed significantly lower AUC signal indicating ACE2 blocking ability of the  
181 immune sera. We then sought to compare how animal sera pools represent blocking ability of  
182 the individual animals. The AUC was calculated for each normalized curve and plotted with the  
183 immunized guinea pig pool AUC. Four of the six guinea pigs immunized against SARS-CoV-2  
184 spike showed statistically significant ACE2 blocking and, importantly, the pooled sera was  
185 comparable to the average AUC from all six sera samples (**Fig. 3F, Fig. S2D**). The competition  
186 ELISA was used to analyze both the IgGs and the sera from the groups, both groups showed  
187 statistically significant blocking of the ACE2 receptor in these assays (**Fig. S2E, Fig. S2F**).

188

#### 189 **Primate serological competition**

190 With the competition ELISA assay demonstrated to be capable of measuring molecular blocking  
191 of the ACE2 receptor in small animals with sera and IgG, we next altered the assay for use with  
192 primate samples. In the small animal studies, the anti-human secondary was used to detect  
193 soluble receptor ACE2-IgHu. However, this secondary antibody would cross-react with  
194 antibodies from primates. To remedy this, an ACE2-mouse Fc fusion (ACE2-IgMu) was utilized  
195 in place of the ACE2-IgHu and an anti-mouse Fc secondary antibody HRP conjugate was used  
196 for detection of ACE2 binding in the presence of primate antibody inhibitors (**Fig. 4A**). To  
197 confirm the function of the replacement ACE2-IgMu, an initial binding ELISA was performed  
198 (**Fig. 4B**). We predicted a similar concentration was needed for optimal competition on the  
199 binding curve (**Fig. 4B, red arrow**) and confirmed this by running a competition ELISA assay

200 using ACE2-IgHu as the competitor at varying ACE2-IgMu constant concentrations (**Fig. 4C**,  
201 **Fig. S3A**). NHP sera from five animals immunized with SARS-CoV-2 spike were pooled and  
202 Day 0 sera from the same group of five animals were pooled as a negative control. The NHP  
203 immune sera displayed appreciable ACE2 blocking compared to the naïve sera (**Fig 4D, Fig.**  
204 **S3B**). Next, we examined if we could detect the presence of receptor blocking antibodies in a  
205 human ICU patient with acute infection. We compared nine positive COVID-19 patients with  
206 sixteen naïve donor samples taken from three years prior to the pandemic. The sera from the  
207 COVID-19 patients was able to block ACE2 receptor binding with statistical significance (**Fig.**  
208 **4E, Fig. S4A**). To compare healthy and COVID-19 patient samples in an independent assay,  
209 we employed a pseudovirus assay we recently developed(23). Sera from the healthy donors  
210 could not neutralize the virus, yet sera from COVID-19 patient samples could neutralize the  
211 virus (**Fig. 4F, Fig S4B, S4C**). This finding is consistent with the ACE2 blocking data and we  
212 show a correlation between pseudovirus neutralization ID50 and AUC for residual ACE2  
213 blocking across all our datasets (**Fig. 5**). Thus, we have demonstrated that the ACE2  
214 competition assay can be employed to measure receptor inhibition levels of human samples.  
215

#### 216 **SPR-based assay for ACE2 receptor blocking**

217 To quantitate blocking of the Spike-ACE2 bimolecular interaction in a second, independent  
218 experiment, we developed a sensitive surface plasmon resonance (SPR) assay. SPR is a  
219 widely used platform that does not require secondary antibodies and therefore we could use a  
220 single assay format for small animals, NHPs and humans. In our assay, a CAP sensor chip is  
221 used to capture single stranded DNA coupled to streptavidin. We are then able to capture  
222 biotinylated spike protein to the surface of the sensor chip (**Fig. 6A**). In SPR, changes in  
223 refractive index occurs when molecules interact with the sensor surface or proteins attach to the  
224 sensor surface and these changes are reported as resonance units (RUs). Next, anti-spike  
225 samples in a dilution series can be injected. After a short time, ACE2 receptor at a constant

226 concentration can be injected to measure residual receptor binding. The change in RUs after  
227 the second injection are a measure of ACE2 blocking.  
228 To demonstrate the feasibility of this assay, we used ACE2-IgHu as both the sample  
229 ( $\text{ACE2}_{\text{sample}}$ ) and the receptor ( $\text{ACE2}_{\text{receptor}}$ ). The sensorgram for this experiment shows  
230  $\text{ACE2}_{\text{sample}}$  injections at various concentrations binding to SARS-CoV-2 RBD between 0 and 125  
231 seconds (**Fig. 6B**). At 225 seconds we inject  $\text{ACE2}_{\text{receptor}}$  at 100nM. We observe  $\text{ACE2}_{\text{receptor}}$   
232 binding to SARS-CoV-2 RBD at the lower  $\text{ACE2}_{\text{sample}}$  concentrations, but not at the highest  
233  $\text{ACE2}_{\text{sample}}$  concentration. The binding signals of  $\text{ACE2}_{\text{sample}}$  and  $\text{ACE2}_{\text{receptor}}$  intersect close to  
234 100nM, suggesting the assay is working as expected (**Fig 6C**). A measure of % ACE2 receptor  
235 inhibition can be calculated to the dose dependence response of the sample (**Fig. 6D**). While  
236 this experiment was done with samples containing a human Fc, this assay can be employed to  
237 measure inhibition of the spike:receptor interaction with any sample regardless of species.

238

## 239 **Discussion**

240 Diagnostic methods that fast and accurately detect functional immunity in a SARS-CoV-2  
241 patient or vaccinee are of critical importance during the global pandemic of 2020. Serological  
242 tests are a central component of our SARS-CoV-2 diagnostic toolbox. Serological tests are  
243 often configured to measure the presence of antibodies that recognize SARS-CoV-2 proteins.  
244 This is not a sufficient measurement to determine if a donor's blood should be used to treat  
245 seriously ill patients or to determine if the donor could be re-infected. Instead, a measurement of  
246 functional antibodies is required. Further, systematic studies of functional antibody responses  
247 and persistence in patients presenting asymptomatic, mild and severe cases will be critical to  
248 understand SARS-CoV-2 immunity. In this study, we developed two new assays which can aid  
249 in understanding the specificity and functionality of antibodies in serum. First, we showed that  
250 an ELISA-based assay could be employed to measure receptor blocking antibodies in animals  
251 vaccinated with SARS-CoV-2 spike protein. We could measure purified IgG or directly from

252 sera, as pools across groups of animals or individual animals. The assay is robust as  
253 exemplified by the ease of adaption to use for five different species. Importantly, the values of  
254 ACE2 blocking measured in our assay correlate with pseudovirus neutralization titers, as seen  
255 in Figure 5. Second, we developed an SPR assay for detecting inhibition of the ACE2 receptor  
256 binding to spike protein.

257

258 Our assays focus on blocking receptor interactions as a surrogate for virus neutralization. In this  
259 study we studied ACE2, because ACE2 appears to be the major receptor for SARS-CoV-2. The  
260 assay could be also be used to study antibodies targeting other coronaviruses with similar  
261 receptors such as SARS-CoV-1 or NL63. The Basigin receptor, as known as CD147, has been  
262 demonstrated to play a role in SARS-CoV-1 infection(24) and is now hypothesized to function in  
263 SARS-CoV-2 invasion of host cells(25). By engineering the ectodomain of CD147 with human  
264 and murine Fc tags, these assays could easily be adapted to study antibody inhibition of  
265 CD147. In addition, antibodies against other coronaviruses, such as MERS, which utilize the  
266 DPP4 receptor could be studied in our assay format using a similar adaptation.

267

268 Neutralizing antibodies can target viral surface proteins to inhibit virus function. Recently, an  
269 antibody (B38) was discovered that can neutralize SARS-CoV-2 and has been structurally  
270 defined to bind to the same site as ACE2(26). In addition, three other antibodies (H4, B5, H2) all  
271 showed neutralizing activity, but B5 and H2 did not compete ACE2 completely, suggesting they  
272 bind an alternative neutralizing epitope on the RBD. In another recent study, a nAb, C12.1,  
273 binds the RBD spike protein, potently neutralizes and protects Syrian hamsters compared to  
274 controls in a passive transfer experiment(27). Recently, a human monoclonal antibody isolated  
275 from transgenic mice (47D11) has been shown to neutralize both SARS-CoV-1 and SARS-CoV-  
2(28). Probing serological responses for competition and blocking of these protective epitopes  
277 could also be easily accomplished through the ELISA and SPR assays reported here.

278

279 The Spike-ACE2 interaction is also being considered as an important therapeutic target. Indeed,  
280 there have been SARS-CoV-1 Spike-ACE2 inhibitors developed previously(29). To examine the  
281 functionality of these small molecules beyond direct binding to the spike protein, assays such as  
282 the one developed here are needed. The SPR instrument is often used for drug discovery and  
283 the SPR assay could be easily adapted to examine blocking capabilities of candidate drugs. The  
284 ELISA assay does not depend on the molecular identity of the competitor, so small molecule or  
285 peptide inhibitors could be directly assessed in this assay.

286

287 Our study presents a new set of assays for assessing ability of antibody samples to inhibit  
288 SARS-CoV-2 Spike interaction with its receptor. As with most assays, the limit of detection can  
289 be an issue. In some of our samples, we saw robust blocking and in others there was minimal  
290 blocking. This could be a property of the samples themselves or a limit in the ability to detect  
291 ACE2 inhibition in our assays. In addition, discovering functional monoclonal antibodies can be  
292 important to understand SARS-CoV-2 immunity and serological assays of functional antibodies  
293 is just a first step. Indeed, a recent report observed that only a small portion of monoclonal  
294 antibodies sorted from convalescent donors are neutralizing(27). Therefore, it is important to  
295 continue to develop and publish assays of varying formats to detect functional antibody  
296 responses in SARS-CoV-2 spike exposed people.

297

## 298 **Conclusions**

299 In a fast-moving global pandemic, we must quickly bring to bear all our immunological  
300 knowledge to create new tools. Receptor-blocking assays can detect functional antibodies in  
301 serum samples. Functional antibody assays can be employed widely to help study SARS-CoV-2  
302 infection, create ‘immune passports’ to enable safe exit from quarantine and for assessing  
303 efficacy of vaccines.

304

305 **Methods**

306

307 **DNA design and plasmid synthesis**

308

309 Protein sequences for human Angiotensin-converting enzyme 2 (huACE2) were obtained  
310 from UniProt (Q9BYF1). DNA encoding the IgG1 human Fc sequence was added to the C-  
311 terminus of the huACE2 and cloned by Twist Bioscience into a modified mammalian pVax-1  
312 expression plasmid to generate the recombinant plasmid, huACE2-IgHu-pVax.

313

314 **Recombinant protein expression and purification**

315

316 Expi293F cells were transfected with plasmid expressing huACE2-IgHu-pVax using PEI/Opti-  
317 MEM. Cell supernatants were harvested 6 days post-transfection by centrifuging (4000xg,  
318 25mins) and filtering (0.2um Nalgene Rapid-flow filter). Supernatants were first purified with  
319 affinity chromatography using AKTA pure 25 system and HiTrap MabSelect SuRe protein A  
320 column (GE healthcare, Cat# 11-0034-94) for huACE2-IgHu-pVax. The eluate fractions from the  
321 affinity purification were pooled, concentrated and dialyzed into 1x PBS buffer before being  
322 further purified by size exclusion chromatography (SEC) using Superdex 200 10/300 GL column  
323 (GE healthcare). Identified SEC eluate fractions were pooled and concentrated to 1mg/mL. The  
324 molecular weight and homogeneity of the purified sample were confirmed through size  
325 exclusion chromatography multi-angle light scattering (SEC MALS) by running the sample in  
326 PBS over Superose 6 increase column followed by DAWN HELEOS II and Optilab T-rex  
327 detectors. The data collected was analyzed using the protein conjugated analysis from ASTRA  
328 software (Wyatt technology).

329

330 **Biophysical characterization of ACE2-IgHu** SPR experiments were performed using a protein  
331 A capture chip on a Biacore 8k. The running buffer was HBS-EP with 1mg/ml BSA. The SARS-  
332 CoV-2 RBD was used as an analyte at concentrations of 100nM, 10nM and 1nM. The  
333 experiment had an association phase for 120sec and the dissociation phase for 600sec. The  
334 data was fit by a 1:1 Langmuir model.

335

336 **SARS-CoV2 Spike binding huACE2-IgHu/ huACE2-IgMu ELISA**

337

338 96-well half area plates (Corning) were coated at room temperature for 8 hours with  
339 1ug/mL PolyRab anti-His antibody (ThermoFisher, PA1-983B), followed by overnight blocking  
340 with blocking buffer containing 1x PBS, 5% skim milk, 1% FBS, and 0.2% Tween-20. The plates  
341 were then incubated with 10ug/mL of SARS-CoV-2, S1+S2 ECD (Sino Biological, 40589-  
342 V08B1) at room temperature for 1-2 hours, followed by addition of either huACE2-IgHu serially  
343 diluted 5-fold (starting concentration, 2ug/mL) or huACE2-IgMu (Sino Biological, 10108-  
344 H05H) serially diluted 5-fold (starting concentration, 50ug/mL). Serial dilutions were performed  
345 using PBS with 1% FBS and 0.2% Tween and incubated at RT for 1 hour. The  
346 plates with huACE2-IgHu were then incubated at room temperature for 1 hour with goat anti-  
347 human IgG-Fc fragment cross adsorbed Ab (Bethyl Laboratories, A80-340P) at 1:10,000  
348 dilution. Similarly, the plates with huACE2-IgMu were incubated with goat anti-mouse IgG H+L  
349 HRP (Bethyl Laboratories, A90-116P) at 1:20,000 dilution. Next, TMB substrate  
350 (ThermoFisher) was added to both plates and then quenched with 1M H<sub>2</sub>SO<sub>4</sub>. Absorbance at  
351 450nm and 570nm were recorded with a BioTek plate reader. Four washes were performed  
352 between every incubation using PBS with 0.05% Tween.

353

354

355

356

357 ***Competition ELISA- Control (huACE2-IgMu Vs huACE2-IgHu)***

358 96-well half area plates (Corning) were coated at room temperature for 8 hours with  
359 1ug/mL PolyRab anti-His antibody (ThermoFisher, PA1-983B), followed by overnight blocking  
360 with blocking buffer containing 1x PBS, 5% skim milk, 1% FBS, and 0.2% Tween-20. The plates  
361 were then incubated with 10ug/mL of SARS-CoV-2, S1+S2 ECD (Sino Biological, 40589-  
362 V08B1) at room temperature for 1-2 hours. huACE2-IgMu (Sino Biological, 10108-  
363 H05H) was serially diluted 3-fold (starting concentration,100ug/mL) with PBS with 1% FBS and  
364 0.2% Tween and pre-mixed with huACE2-IgHu at constant concentrations (ranging from 0.01-  
365 10ug/mL) The pre-mixture was then added to the plate and incubated at RT for 1 hour. The  
366 plates were further incubated at room temperature for 1 hour with goat anti-human IgG-Fc  
367 fragment cross adsorbed Ab (Bethyl Laboratories, A80-340P) at 1:10,000 dilution, followed by  
368 addition of TMB substrate (ThermoFisher) and then quenched with 1M H<sub>2</sub>SO<sub>4</sub>. Absorbance at  
369 450nm and 570nm were recorded with a BioTek plate reader. Four washes were performed  
370 between every incubation using PBS with 0.05% Tween.

371

372

373 ***Competition ELISA- Mouse***

374 IgG was purified from sera taken from mice immunized with SARS-CoV-2 Spike protein (INO-  
375 4800) (23) using Nab protein G spin kit (ThermoFisher, 89949). 96-well half area plates  
376 (Corning) were coated at room temperature for 8 hours with 1ug/mL PolyRab anti-His antibody  
377 (ThermoFisher, PA1-983B), followed by overnight blocking with blocking buffer containing 1x  
378 PBS, 5% skim milk, 1% FBS, and 0.2% Tween-20. The plates were then incubated with  
379 10ug/mL of SARS-CoV-2, S1+S2 ECD (Sino Biological, 40589-V08B1) at room temperature  
380 for 1-2 hours. Purified IgG was serially diluted 3-fold (starting concentration,100ug/mL) with PBS  
381 with 1% FBS and 0.2% Tween and pre-mixed with huACE2-IgHu at constant

382 concentration of 0.1ug/mL. The pre-mixture was then added to the plate and incubated at RT  
383 for 1 hour. The plates were further incubated at room temperature for 1 hour with goat anti-  
384 human IgG-Fc fragment cross adsorbed Ab (Bethyl Laboratories, A80-340P) at 1:10,000  
385 dilution, followed by addition of TMB substrate (ThermoFisher) and then quenched with 1M  
386 H<sub>2</sub>SO<sub>4</sub>. Absorbance at 450nm and 570nm were recorded with a BioTek plate reader. Four  
387 washes were performed between every incubation using PBS with 0.05% Tween.

388

389

390 ***Competition ELISA- Guinea pig***

391 Sera from guinea pigs immunized with INO-4800(23) was collected and pooled together prior to  
392 immunization (Day 0, n=5) and two weeks post immunization. Sera from naïve guinea pigs  
393 (n=5) given a saline control was also pooled. IgG was purified from these sera pools using Nab  
394 protein A/G spin kit (Cat# Thermo, 89950 ). 96-well half area plates (Corning) were coated at  
395 room temperature for 8 hours with 1ug/mL PolyRab anti-His antibody (ThermoFisher, PA1-  
396 983B), followed by overnight blocking with blocking buffer containing 1x PBS, 5% skim milk, 1%  
397 FBS, and 0.2% Tween-20. The plates were then incubated with 10ug/mL of SARS-CoV-2,  
398 S1+S2 ECD (Sino Biological, 40589-V08B1) at room temperature for 1-2 hours. Either purified  
399 sera or IgG (Day0, Day14 or naïve) was serially diluted 3-fold with PBS with 1% FBS and 0.2%  
400 Tween and pre-mixed with huACE2-IgHu at a constant concentration of 0.1ug/mL. The pre-  
401 mixture was then added to the plate and incubated at RT for 1 hour. The plates  
402 were further incubated at room temperature for 1 hour with goat anti-human IgG-Fc fragment  
403 cross adsorbed Ab (Bethyl Laboratories, A80-340P) at 1:10,000 dilution, followed by addition of  
404 TMB substrate (ThermoFisher) and then quenched with 1M H<sub>2</sub>SO<sub>4</sub>. Absorbance at 450nm and  
405 570nm were recorded with a BioTek plate reader. Four washes were performed between every  
406 incubation using PBS with 0.05% Tween.

407

408

409 ***Competition ELISA- Rabbit***

410 Rabbits were immunized with 1mg or 2mg of ION-4800 at Day 0 and Week 4. Sera from  
411 immunized rabbits was collected and pooled together prior to immunization (Day 0, n=5) and 2  
412 weeks post 2nd immunization (wk 6, n=5), (Patel A. et al., in preparation). Sera from naïve  
413 rabbits (n=5) given a saline control was also pooled. IgG was purified from these sera pools  
414 using Nab protein A/G spin kit (Thermo, 89950). 96-well half area plates (Corning) were coated  
415 at room temperature for 8 hours with 1ug/mL PolyRab anti-His antibody (ThermoFisher, PA1-  
416 983B), followed by overnight blocking with blocking buffer containing 1x PBS, 5% skim milk, 1%  
417 FBS, and 0.2% Tween-20. The plates were then incubated with 10ug/mL of SARS-CoV-2,  
418 S1+S2 ECD (Sino Biological, 40589-V08B1) at room temperature for 1-2 hours. Either sera  
419 pool or purified IgG (IgGr) from Day0, low dose, high dose or naïve animals was serially  
420 diluted 3-fold with PBS with 1% FBS and 0.2% Tween and pre-mixed with huACE2-IgHu at  
421 constant concentration of 0.1ug/mL. The pre-mixture was then added to the plate  
422 and incubated at RT for 1 hour. The plates were further incubated at room temperature for 1  
423 hour with goat anti-human IgG-Fc fragment cross adsorbed Ab (Bethyl Laboratories, A80-340P)  
424 at 1:10,000 dilution, followed by addition of TMB substrates (ThermoFisher) and then quenched  
425 with 1M H<sub>2</sub>SO<sub>4</sub>. Absorbance at 450nm and 570nm were recorded with a BioTek plate  
426 reader. Four washes were performed between every incubation using PBS with 0.05% Tween.  
427  
428

429 ***Competition ELISA- Primates***

430 Rhesus macaques were immunized with 1mg of INO-4800 at Day 0 and Week 4. Sera from  
431 immunized NHPs was collected and pooled together prior to immunization (Day 0, n=5) and 2  
432 weeks post 2nd immunization (Wk 6, n=5), (Patel A. et al., in preparation). Sera from SARS-  
433 CoV-2 positive patients treated at the Hospital of the University of Pennsylvania was also

434 collected and compared to sera from healthy human donors purchased from BioChemied in  
435 December of 2016, well before the SARS-CoV-2 pandemic. 96-well half area plates (Corning)  
436 were coated at 4°C overnight with 1ug/mL of SARS-CoV-2, S1+S2 ECD (Sino Biological,  
437 40589-V08B1). Plates were washed 4x with 1x PBS, 0.05% Tween-20 using a plate washer,  
438 and then blocked with 1x PBS, 5% skim milk, 0.1% Tween-20 at room temperature for 1 hour.  
439 After washing, sera was serially diluted 3-fold in 1x PBS, 5% skim milk, 0.1% Tween-20 and  
440 incubated on the plate at room temperature for 1 hour. Plates were washed, then incubated with  
441 a constant concentration of 0.4 ug/mL huACE2-IgMu diluted in 1x PBS, 5% skim milk, 0.1%  
442 Tween-20 at room temperature for 1 hour. After washing, plates were further incubated at room  
443 temperature for 1 hour with goat anti-mouse IgG H+L HRP (Bethyl Laboratories, A90-116P) at  
444 1:20,000 dilution in 1x PBS, 5% skim milk, 0.1% Tween-20. Plates were then washed, followed  
445 by addition of TMB substrate (ThermoFisher) and then quenched with 1M H<sub>2</sub>SO<sub>4</sub>. Absorbance at  
446 450nm and 570nm were recorded with a BioTek plate reader. Four washes were performed  
447 between every incubation using PBS with 0.05% Tween.

448

449

#### 450 **SPR Assay**

451 Surface Plasmon Resonance experiments were conducted on a Biacore 8K instrument. The  
452 running and dilution buffers were HBS-EP, 1 mg/ml BSA, 0.05% Tween. Biotin CAPture reagent  
453 was injected over the Series S CAP Sensor chip (Cytiva Life Sciences 28920234) at 2 ul/min for  
454 300s. Followed by capture of SARS-CoV-2 receptor binding domain which was biotinylated  
455 using the lightning-link type-A biotinylation kit(Expedeon/Abcam, 370-0005) for 180s at  
456 10ul/min. Next, the sample (ACE2-IgHu) at 8 concentrations of 1500nM to 0.7nM. The  
457 association was for 120s second at a flow rate of 30 ul/min and followed by a short dissociation  
458 time of 15s. A constant ACE2-IgHu was injected at 100 nM in each flow cell for 120s followed by  
459 60s dissociation at a flow rate of 30ul/min. The difference in response units before injection and

460 after dissociation of the sample application and the constant receptor was calculated for each  
461 curve. The regeneration solution was made using 3-parts 8M guanidine hydrochloride and 1-  
462 part 1M sodium hydroxide.

463

#### 464 **Statistics**

465 Statistical analyses were performed using GraphPad Prism 8 software. The data were considered  
466 significant if  $p < 0.05$ . The lines in all graphs represent the mean value and error bars represent  
467 the standard deviation. The AUC values were normalized as a percentage of Day 0 AUC. No  
468 samples were excluded from the analysis. Samples were not blinded before performing each  
469 experiment.

470

#### 471 **SARS-CoV-2 Pseudovirus assay**

472 The SARS-CoV-2 pseudovirus was produced by co-transfection of HEK293T cells with 1:1 ratio  
473 of DNA plasmid encoding SARS-CoV-2 S protein (GenScript) and backbone plasmid pNL4-  
474 3.Luc.R-E- (NIH AIDS Reagent) using GeneJammer (Agilent) in 10% FBS/DMEM enriched  
475 with 1% Penicillin/Streptomycin (D10 medium). The supernatant containing pseudovirus was  
476 harvested 48 hours post-transfection and enriched with FBS to 12% total volume, sterifiltered  
477 and stored at -80C. The pseudovirus was tittered using a stable ACE2-293T cell line that had  
478 previously been generated(23). For neutralization assay, serially diluted samples were incubated  
479 with pseudovirus at room temperature for 90 minutes and added to 10,000 ACE2-293T cells in  
480 200uL TPCK media (DMEM supplemented with 1%BSA, 25mM HEPES, 1ug/ml of TPCK and 1X  
481 Penicillin-Streptomycin) in 96-well tissue culture plates, and incubated at 37C and 5% CO<sub>2</sub> for  
482 72 hours. The cells were subsequently harvested and lysed with BriteLite reagent (PerkinElmer),  
483 and luminescence from the plates were recorded with a BioTek plate reader.

484

485 **Availability of data and materials**

486 The data are available from the corresponding author upon request.

487

488 **Abbreviations**

489 **References**

- 490 1. Li R, Pei S, Chen B, Song Y, Zhang T, Yang W, et al. Substantial undocumented infection  
491 facilitates the rapid dissemination of novel coronavirus (SARS-CoV-2). *Science*.  
492 2020;368(6490):489-93.
- 493 2. Dong E, Du H, Gardner L. An interactive web-based dashboard to track COVID-19 in real  
494 time. *Lancet Infect Dis*. 2020;20(5):533-4.
- 495 3. Li W, Moore MJ, Vasilieva N, Sui J, Wong SK, Berne MA, et al. Angiotensin-converting  
496 enzyme 2 is a functional receptor for the SARS coronavirus. *Nature*. 2003;426(6965):450-4.
- 497 4. Zhou P, Yang XL, Wang XG, Hu B, Zhang L, Zhang W, et al. A pneumonia outbreak  
498 associated with a new coronavirus of probable bat origin. *Nature*. 2020;579(7798):270-3.
- 499 5. Xiao X, Chakraborti S, Dimitrov AS, Gramatikoff K, Dimitrov DS. The SARS-CoV S  
500 glycoprotein: expression and functional characterization. *Biochem Biophys Res Commun*.  
501 2003;312(4):1159-64.
- 502 6. Lan J, Ge J, Yu J, Shan S, Zhou H, Fan S, et al. Structure of the SARS-CoV-2 spike receptor-  
503 binding domain bound to the ACE2 receptor. *Nature*. 2020.
- 504 7. Shang J, Ye G, Shi K, Wan Y, Luo C, Aihara H, et al. Structural basis of receptor  
505 recognition by SARS-CoV-2. *Nature*. 2020;581(7807):221-4.
- 506 8. Tai W, He L, Zhang X, Pu J, Voronin D, Jiang S, et al. Characterization of the receptor-  
507 binding domain (RBD) of 2019 novel coronavirus: implication for development of RBD protein  
508 as a viral attachment inhibitor and vaccine. *Cell Mol Immunol*. 2020.
- 509 9. Wan Y, Shang J, Graham R, Baric RS, Li F. Receptor Recognition by the Novel Coronavirus  
510 from Wuhan: an Analysis Based on Decade-Long Structural Studies of SARS Coronavirus. *J Virol*.  
511 2020;94(7).
- 512 10. Yan R, Zhang Y, Li Y, Xia L, Guo Y, Zhou Q. Structural basis for the recognition of SARS-  
513 CoV-2 by full-length human ACE2. *Science*. 2020;367(6485):1444-8.
- 514 11. Wrapp D, Wang N, Corbett KS, Goldsmith JA, Hsieh CL, Abiona O, et al. Cryo-EM  
515 structure of the 2019-nCoV spike in the prefusion conformation. *Science*. 2020;367(6483):1260-  
516 3.
- 517 12. Walls AC, Park YJ, Tortorici MA, Wall A, McGuire AT, Veesler D. Structure, Function, and  
518 Antigenicity of the SARS-CoV-2 Spike Glycoprotein. *Cell*. 2020;181(2):281-92 e6.
- 519 13. Zhang JS, Chen JT, Liu YX, Zhang ZS, Gao H, Liu Y, et al. A serological survey on  
520 neutralizing antibody titer of SARS convalescent sera. *J Med Virol*. 2005;77(2):147-50.
- 521 14. Shen C, Wang Z, Zhao F, Yang Y, Li J, Yuan J, et al. Treatment of 5 Critically Ill Patients  
522 With COVID-19 With Convalescent Plasma. *JAMA*. 2020.

- 523 15. Duan K, Liu B, Li C, Zhang H, Yu T, Qu J, et al. Effectiveness of convalescent plasma  
524 therapy in severe COVID-19 patients. Proc Natl Acad Sci U S A. 2020;117(17):9490-6.
- 525 16. Harvala H, Robb M, Watkins N, Ijaz S, Dicks S, Patel M, et al. Convalescent plasma  
526 therapy for the treatment of patients with COVID-19: Assessment of methods available for  
527 antibody detection and their correlation with neutralising antibody levels. medRxiv.  
528 2020:2020.05.20.20091694.
- 529 17. Chen WH, Strych U, Hotez PJ, Bottazzi ME. The SARS-CoV-2 Vaccine Pipeline: an  
530 Overview. Curr Trop Med Rep. 2020:1-4.
- 531 18. Shirato K, Nao N, Katano H, Takayama I, Saito S, Kato F, et al. Development of Genetic  
532 Diagnostic Methods for Novel Coronavirus 2019 (nCoV-2019) in Japan. Jpn J Infect Dis. 2020.
- 533 19. Krammer F, Simon V. Serology assays to manage COVID-19. Science. 2020.
- 534 20. Lassaunière R, Frische A, Harboe ZB, Nielsen AC, Fomsgaard A, Krogfelt KA, et al.  
535 Evaluation of nine commercial SARS-CoV-2 immunoassays. medRxiv.  
536 2020:2020.04.09.20056325.
- 537 21. Nie J, Li Q, Wu J, Zhao C, Hao H, Liu H, et al. Establishment and validation of a  
538 pseudovirus neutralization assay for SARS-CoV-2. Emerg Microbes Infect. 2020;9(1):680-6.
- 539 22. Masson JF. Portable and field-deployed surface plasmon resonance and plasmonic  
540 sensors. Analyst. 2020.
- 541 23. Smith TRF, Patel A, Ramos S, Elwood D, Zhu X, Yan J, et al. Immunogenicity of a DNA  
542 vaccine candidate for COVID-19. Nat Commun. 2020;11(1):2601.
- 543 24. Chen Z, Mi L, Xu J, Yu J, Wang X, Jiang J, et al. Function of HAb18G/CD147 in invasion of  
544 host cells by severe acute respiratory syndrome coronavirus. J Infect Dis. 2005;191(5):755-60.
- 545 25. Wang K, Chen W, Zhou Y-S, Lian J-Q, Zhang Z, Du P, et al. SARS-CoV-2 invades host cells  
546 via a novel route: CD147-spike protein. bioRxiv. 2020:2020.03.14.988345.
- 547 26. Wu Y, Wang F, Shen C, Peng W, Li D, Zhao C, et al. A noncompeting pair of human  
548 neutralizing antibodies block COVID-19 virus binding to its receptor ACE2. Science. 2020.
- 549 27. Zost SJ, Gilchuk P, Chen R, Case JB, Reidy JX, Trivette A, et al. Rapid isolation and  
550 profiling of a diverse panel of human monoclonal antibodies targeting the SARS-CoV-2 spike  
551 protein. bioRxiv. 2020:2020.05.12.091462.
- 552 28. Wang C, Li W, Drabek D, Okba NMA, van Haperen R, Osterhaus A, et al. A human  
553 monoclonal antibody blocking SARS-CoV-2 infection. Nat Commun. 2020;11(1):2251.
- 554 29. Huentelman MJ, Zubcevic J, Hernandez Prada JA, Xiao X, Dimitrov DS, Raizada MK, et al.  
555 Structure-based discovery of a novel angiotensin-converting enzyme 2 inhibitor. Hypertension.  
556 2004;44(6):903-6.
- 557

558

## 559 **Acknowledgements**

560 The authors would like to Matthew Sullivan for providing feedback on the manuscript.

## 561 **Funding**

562 This work was supported by grant from the Coalition for Epidemic Preparedness Innovations  
563 (CEPI).

564

565 **Contributions**

566 S.W., N.C. and D.W.K.: Developed the receptor-blocking assays. Designed and characterized  
567 ACE2-IgHu protein and the SARS-CoV-2 RBD protein. Planned and executed the experiments  
568 and analyzed the data. E.L.R. and K.Y.K.: optimized, planned and executed the experiments  
569 involving the human samples. E.L.R., E.G., A.P., P.T.: produced reagents. M. P. and Z.X.  
570 created and executed the pseudovirus neutralization assay. S.W., N.C. and D.W.K. wrote the  
571 paper. E.L.R., E.G., M.P., Z.X., A.P., D.B.W. helped write the paper.

572

573 **Declarations**

574 **Ethics approval and consent to participate**

575 N/A - This study did not require ethics approval and consent.

576 **Consent for publication**

577 N/A – no identifiable information was included.

578 **Competing interests**

579 T.S. and K.S. are employees of Inovio Pharmaceuticals and as such receive salary and  
580 benefits, including ownership of stock and stock options, from the company. D.B.W. has  
581 received grant funding, participates in industry collaborations, has received speaking honoraria,  
582 and has received fees for consulting, including serving on scientific review committees and  
583 board services. Remuneration received by D.B.W. includes direct payments or stock or stock  
584 options, and in the interest of disclosure he notes potential conflicts associated with this work

585 with Inovio and possibly others. In addition, he has a patent DNA vaccine delivery pending to  
586 Inovio. All other authors report there are no competing interests.

587

588 **Additional information**

589

590

591 **Figure Legends**

592 **Figure 1. ACE2 receptor expression and affinity.** **a)** UV trace from SEC of ACE2-IgHu  
593 expressed in mammalian cells and purified on a protein A column **b)** SEC-MALS determined  
594 molecular weight of ACE2-IgHu to be that of a dimeric complex (~190kDa) as shown by the line  
595 under the peak on the right y-axis **c)** Affinity of SARS CoV-2 receptor binding domain for  
596 immobilized ACE2-IgHu assessed by SPR (27nM) curves are concentrations of RBD X, Y, and  
597 Z **d)** Affinity of ACE2-IgHu for immobilized SARS CoV-2 full-length spike protein assessed by  
598 ELISA. Optimal concentration of ACE2-IgHu for competition assays (~EC<sub>90</sub>, red arrow) requires  
599 high signal without excess receptor present

600

601 **Figure 2. ACE2 receptor competition assay development.** **a)** Competition ELISA schematic  
602 displaying immobilized anti-His pAb (red) capturing His6X-tagged SARS-CoV-2 spike protein  
603 (rainbow). Premixed ACE2-IgHu (green, blue) at a constant concentration with a dilution series  
604 of competitors (green, red) is added and anti-human-HRP (green) determines amount of ACE2-  
605 IgHu remaining in the presence of competitors through a colorimetric readout **b)** Four constant  
606 concentrations of ACE2-IgHu were tested with varying concentrations of the ACE2-IgMu  
607 competitor to establish an optimal ACE2-IgHu concentration which displays a full blocking curve  
608 (red, 0.10ug/ml) from the competitor dilution series while retaining a wide range in signal.

609

610 **Figure 3. Animal IgG and serological competition.** **a)** IgG and serological competition  
611 schematic. Anti-his pAb captures CoV-2 spike protein. Immunized sera or IgG from small  
612 animals are used as competitors to block ACE2-IgHu receptor binding when premixed. ACE2-  
613 IgHu remaining is determined from an anti-human-HRP colorimetric readout **b)** IgGs present in  
614 a vaccinated BALB/c mouse block ACE2-IgHu binding with greater effect when full-length  
615 SARS-CoV-2 S1-S2 spike protein is immobilized versus the S1 subunit by itself **c)** Area Under  
616 the Curve (AUC) schematic displaying the larger area for uninhibited ACE2 binding versus the  
617 area from curves showing competition with ACE2 **d)** AUC of IgGs purified from immunized  
618 rabbit sera (IgGr low dose, blue; IgGr high dose, red) vs naïve IgGr or Day 0 IgGr. **e)** AUC of  
619 sera from immunized rabbits (low dose Rabbit sera, blue; high dose Rabbit sera, red) versus  
620 naïve Rabbit sera or Day 0 Rabbit sera. **f)** AUC of sera from immunized guinea pigs at week 2  
621 (dark blue) and individual animals (blue), naïve sera (grey) and pooled Day 0 sera from all  
622 animals (black). The pooled immunized curve displayed a comparable AUC to the average AUC  
623 from all individual immunized animals.

624

625 **Figure 4. Primate serological competition.** **a)** Competition ELISA schematic displaying  
626 immobilized His6X-tagged CoV-2 spike protein (rainbow). Preblocking of the spike protein with  
627 primate sera (blue) at varying concentrations was added followed by ACE2-IgMu (green, blue)  
628 at a constant concentration. Anti-mouse-HRP (green) determines amount of ACE2-IgMu  
629 remaining in the presence of competitors through a colorimetric readout **b)** Affinity of ACE2-  
630 IgMu for immobilized SARS CoV-2 S1+S2 full-length spike protein assessed by ELISA. Optimal  
631 concentration of ACE2-IgMu for competition assays (red arrow, 0.4ug/ml) requires high signal  
632 without excess receptor present. **c)** Optimal ACE2-IgMu concentration which displays a full  
633 blocking curve (0.40ug/ml) from the competitor dilution series (ACE2-IgHu) while retaining a  
634 wide range in signal **d)** NHP sera pooled from five vaccinated animals was used as competitors  
635 in the primate competition assay. The AUC from vaccinated NHP sera (blue) versus Day 0 NHP

636 sera (black). **e)** Human sera from nine SARS-CoV-2 positive COVID-19 patients was tested in  
637 the primate competition assay and compared to sixteen naïve human sera collected pre-  
638 pandemic. The AUC of the COVID-19 patient serum (purple) is significantly decreased  
639 compared to the pre-pandemic human serum (grey). **f)** Human sera was analyzed by a  
640 pseudovirus neutralization assay. The samples and the coloring are the same as in e).

641

642

643 **Figure 5. ACE2 receptor blocking correlates with psuedovirus neuralization.** A symbol  
644 represents each of the individual datapoints where we had a paired AUC blocking and  
645 pseudovirus ID50 values. The human samples are in triangles, the mice in circles, individual  
646 Guniea pigs in squares, Guniea pig pools in diamonds and rabbit pools in hexagons. SARS-  
647 CoV-2 spike experienced samples are shown in color. Naïve samples and healthy donors are  
648 shown in grey. Least-squares fit line is shown with p-value and R squared from Prism.

649

650 **Figure 6. ACE2 receptor competition assay development.** **a)** Overview of SPR experiment  
651 depicting SARS-CoV-2 capture by streptavidin-biotin interaction, sera injected as analyte and  
652 ACE2 injected as second analyte **b)** Sensorgram for ACE2 blocking SPR assay ACE2-IgHu  
653 injected as sample as indicated and ACE-IgHu injected as receptor as indicated. Sample  
654 responses were referenced to blank injections. **c)** Response in RUs measured at the end of  
655 sample injection (blue) and receptor injection (red) at each concentration of sample. **d)** ACE2  
656 inhibition curve derived from RUs at each concentration

657

658 **Supplemental Figs**

659

660 **Supplemental Figure 1. ACE2 receptor expression and assay development.**

661 a) ACE2-IgHu binding comparison for immobilized S1 spike protein from varying batches of  
662 expression and purification as well as freeze-thaw assessment via ELISA show negligible  
663 differences.

664

665 **Supplemental Figure 2. Animal IgG and serological competition.** a) AUC is significantly  
666 decreased in the presence of vaccinated mouse IgG competitors; however a greater decrease  
667 is observed when full-length CoV-2 spike protein was immobilized versus naïve mouse IgG  
668 samples. b) ELISA competition curves for vaccinated rabbit IgG (IgGr low dose, blue; IgGr high  
669 dose, red) or sera (sera low dose, blue; sera high dose, red) versus naïve rabbit IgG or c) sera  
670 samples (grey) and pooled Day 0 rabbit IgG or sera samples (black). d) ELISA competition  
671 curves for Week 2 vaccinated guinea pig sera (pool, dark blue; individual animals, blue) versus  
672 naïve guinea pig sera samples (grey) and pooled prevaccinated guinea pig sera samples  
673 (black). e) AUC for vaccinated guinea pig IgG pool (blue) versus naïve guinea pig IgG pool  
674 (grey) and pooled prevaccinated guinea pig IgG samples (black) f) ELISA competition curves  
675 with same coloring as in e.

676

677 **Supplemental Figure 3. Primate serological competition.** a) Four constant concentrations of  
678 ACE2-IgMu were tested with varying concentrations of the ACE2-IgHu competitor to establish  
679 an optimal ACE2-IgMu concentration which displays a full blocking curve (red, 1.0ug/ml) from  
680 the competitor dilution series while retaining a wide range in signal. b) ELISA competition  
681 curves for vaccinated NHP sera (blue) versus pooled Day 0 NHP sera (black).

682

683 **Supplemental Figure 4. a)** Human sera from nine SARS-CoV-2 positive COVID-19 patients  
684 was tested in the primate competition assay and compared to sixteen naïve human sera  
685 collected pre-pandemic. The AUC of the COVID-19 patient serum (purple) is significantly  
686 decreased compared to the pre-pandemic human serum (grey) and normalized to a buffer

687 control. **b)** pseudovirus neutralization assay for the nine SARS-CoV-2 positive COVID-19  
688 patients displayed neutralization for all samples to varying degrees **c)** pseudovirus neutralization  
689 assay for the sixteen naïve human sera collected pre-pandemic displayed little to no  
690 neutralization for all samples.

691

692

693

694

Figure 1

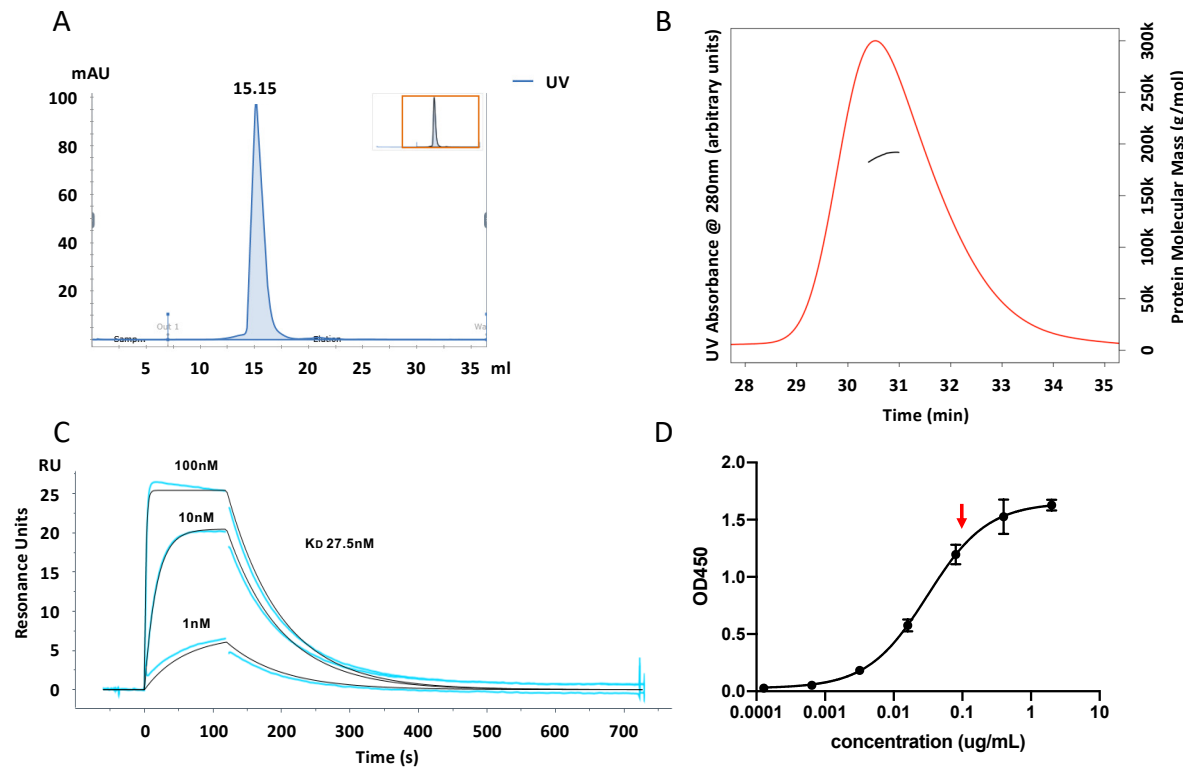


Figure 2

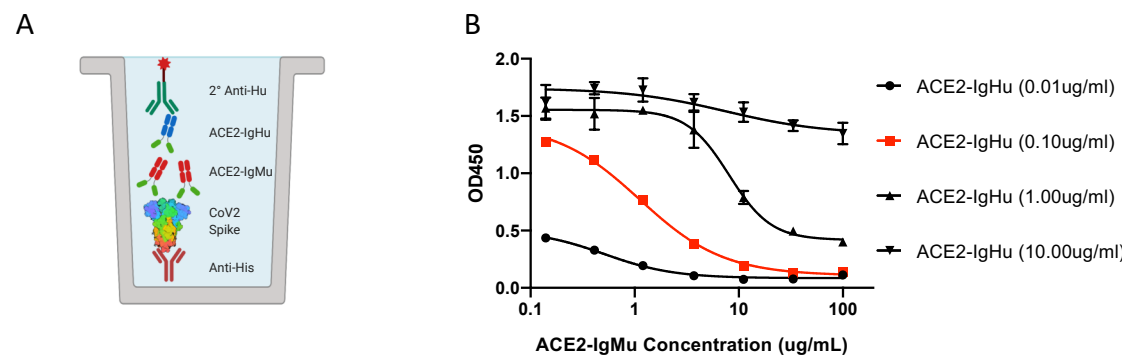


Figure 3

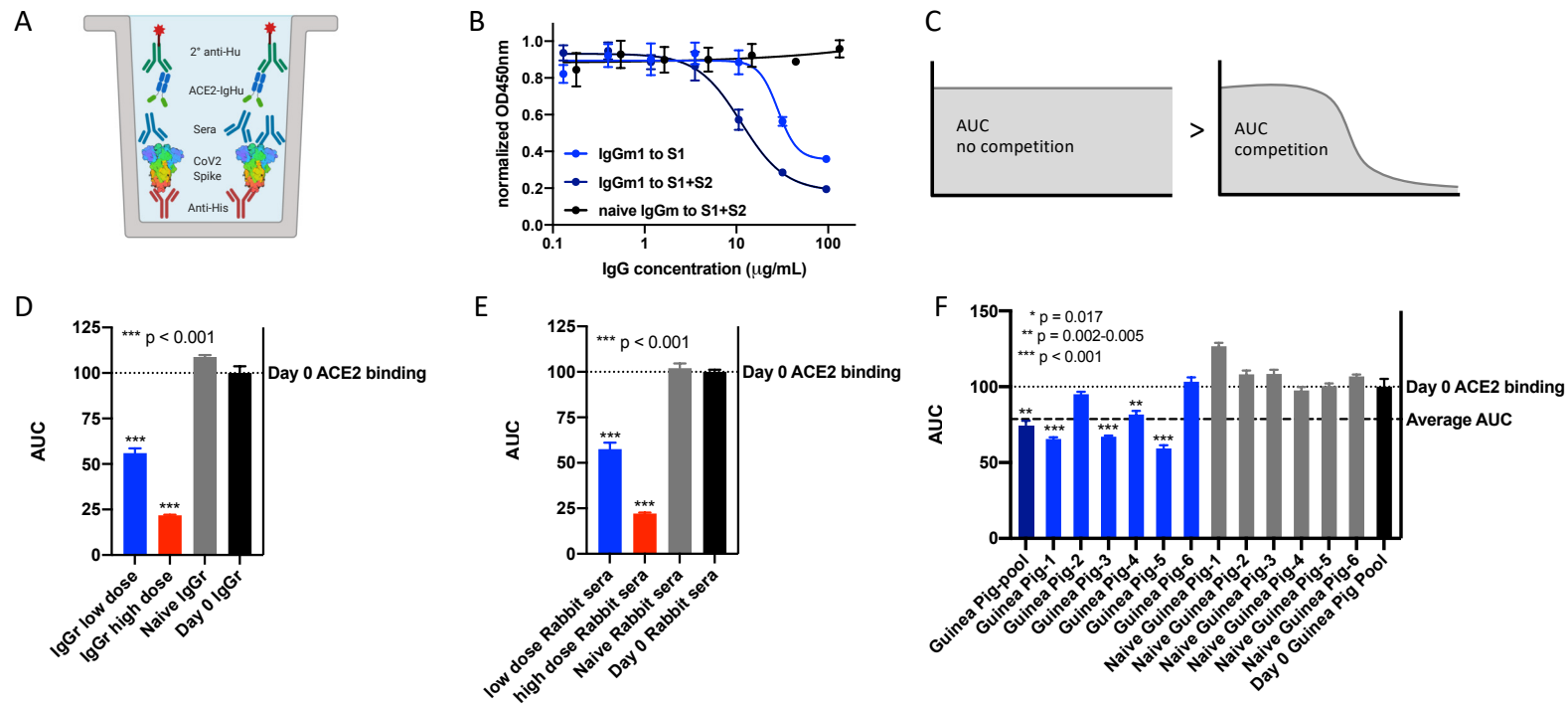


Figure 4

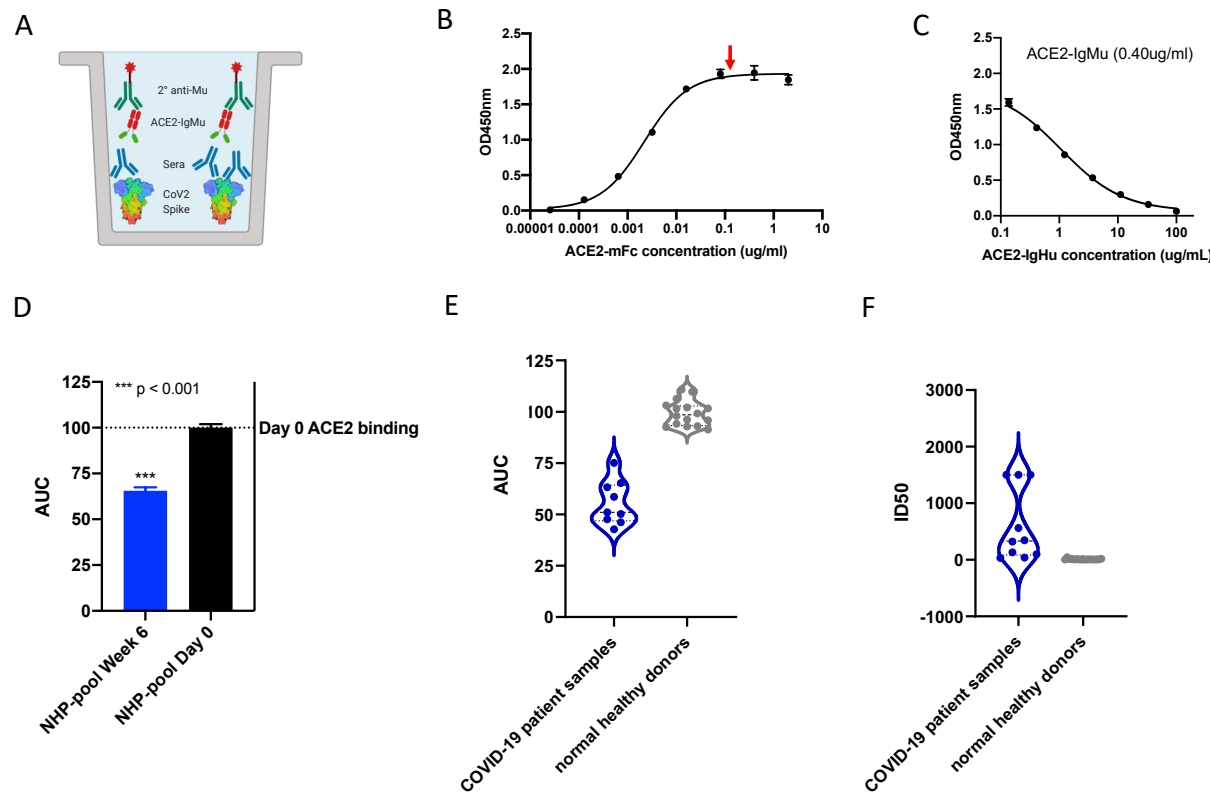


Figure 5

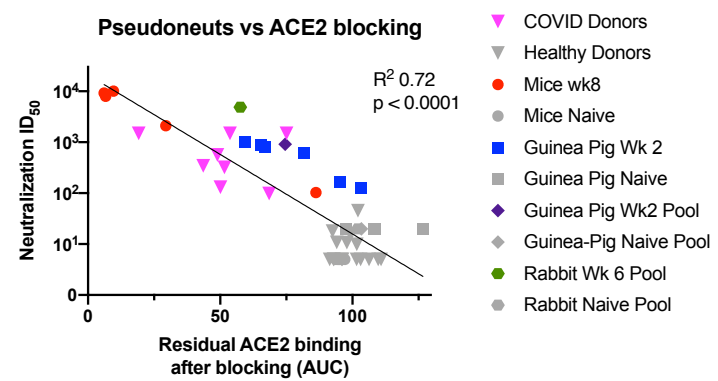


Figure 6

